How expectations of pain elicited by consciously and unconsciously perceived cues unfold over time

Yiheng Tu[a,d], **Dimitrios Pantazis**[b,c], **Georgia Wilson**[a], **Sheraz Khan**[d], **Seppo Ahlfors**[d], **Jian Kong**[a,d,*]

[a]Department of Psychiatry, Massachusetts General Hospital and Harvard Medical School, Charlestown, MA, USA

[b]Department of Brain and Cognitive Sciences, Massachusetts Institute of Technology, Cambridge, MA, USA

[c]McGovern Institute of Brain Research, Massachusetts Institute of Technology, Cambridge, MA, USA

[d]Athinoula A. Martinos Center for Biomedical Imaging, Massachusetts General Hospital and Harvard Medical School, Charlestown, MA, USA

Abstract

Expectation can shape the perception of pain within a fraction of time, but little is known about how perceived expectation unfolds over time and modulates pain perception. Here, we combine magnetoencephalography (MEG) and machine learning approaches to track the neural dynamics of expectations of pain in healthy participants with both sexes. We found that the expectation of pain, as conditioned by facial cues, can be decoded from MEG as early as 150 ms and up to 1100 ms after cue onset, but decoding expectation elicited by unconsciously perceived cues requires more time and decays faster compared to consciously perceived ones. Also, results from temporal generalization suggest that neural dynamics of decoding cue-based expectation were predominately sustained during cue presentation but transient after cue presentation. Finally, although decoding expectation elicited by consciously perceived cues were based on a series of time-restricted brain regions during cue presentation decoding relied on the medial prefrontal cortex and anterior cingulate cortex after cue presentation for both consciously and unconsciously perceived cues. These findings reveal the conscious and unconscious processing of expectation

during pain anticipation and may shed light on enhancing clinical care by demonstrating the impact of expectation cues.

Keywords

1. Introduction

Pain is a highly subjective sensation that can be influenced by a variety of psychological factors (Wiech et al., 2008). One such example is that our expectations can significantly modulate the perception of pain (Atlas and Wager, 2012; Fields, 2018), and these modulation effects (e.g., placebo analgesia and nocebo hyperalgesia) have been robustly observed in both basic and clinical studies (Finniss et al., 2010; Kong et al., 2009; Kong et al., 2018). In the case of placebo analgesia, classical theories invoke conditioning to establish a link between a cue (e.g., pain killer) and the following pain relief, thus creating predictive knowledge (i.e., expectation) that modulates future pain-related responses to the same cue, even if it is inert (Kong and Benedetti, 2014).

Although the mechanisms of placebo and nocebo are still under investigation, neuroimaging techniques, especially functional magnetic resonance imaging (fMRI) and positron emission tomography (PET), have offered insights into how predictive cues are processed by higher-order brain areas (Atlas et al., 2010; Petrovic et al., 2010; Tu et al., 2020; Wager et al., 2004) and then modulate pain and pain-related brain responses (Freeman et al., 2015; Wager and Atlas, 2015). These theories have been recently extended to propose that predictive cues can be recognized subliminally and conditioned pain-related responses (e.g., placebo analgesia and nocebo hyperalgesia) can be elicited without conscious awareness (Jensen et al., 2015, 2012), but placebo and nocebo effects induced by unconsciously perceived cues may be weaker than conscious ones (Egorova et al., 2015; Tu et al., 2018).

Knowing how the human brain extracts expectation from predictive cues is important for understanding and harnessing placebo and nocebo effects. However, there are critical gaps of knowledge in this domain. First, previous studies using fMRI have had low temporal resolution and were not able to track neural dynamics at the level of milliseconds (Wager et al., 2004). When and how expectations are extracted, evaluated, and maintained after predictive cue onset are still unknown. Second, studies suggested that visual percept could be processed in the brain without conscious awareness (King et al., 2016; Salti et al., 2015). Whether expectation elicited by consciously and unconsciously perceived visual cues during pain anticipation are associated with distinct neural dynamics remains unclear.

To answer these questions, we leveraged a visual cue conditioning paradigm with both consciously and unconsciously perceived predictive facial cues and collected magnetoencephalography (MEG) data during the experiment. In the conditioning phase, cue-based expectations of pain were both directly and indirectly conditioned (viewing a model participant undergoing direct conditioning rather than receiving pain themselves) for

all participants (this setup allows us to explore possible effect of conditioning type on time-resolved expectations, since recent studies showed that expectations of pain could be conditioned by both self-experience and social observation (Schenk and Colloca, 2020; Tu et al., 2018)). In the test phase, to determine how cue-based expectation of pain unfolds over time, we focused on analyzing the MEG data from subjects viewing other conditioned cues, which were supraliminally and subliminally presented, to the onset of identical pain stimuli (i.e., pain anticipatory period). We applied multivariate pattern classification on MEG sensor measurements to decode levels of cue-based expectation (i.e., high pain vs. low pain) along with time, and then compared the neural dynamics for decoding expectations elicited by consciously and unconsciously perceived cues. Finally, we examined how these neural dynamics mediated expectation of subjective pain intensities. We hypothesized that (1) participants would report significantly different levels of pain perception following different cues, even the intensity of pain stimuli were identical; (2) decoding consciously and unconsciously perceived expectations would be associated with distinct spatiotemporal neural patterns; and (3) conditioning types (direct vs indirect) would not affect the decoding process.

2. Methods

2.1. Subjects

Thirty-seven healthy individuals without psychiatric or neurologic disorders took part in this study. Fourteen subjects were dropped from study; seven due to interference in the MEG scanner, two due to inability to recognize facial cues, four due to inconsistent pain ratings, and one due to reported back pain. Two subjects were unable to complete the experiment. The final sample consisted of 21 participants (12 females; aged 25.0 ± 3.9). The Massachusetts General Hospital Institutional Review Board approved the study, and all subjects provided written informed consent.

2.2. Pain administration

A PATHWAY contact heat-evoked potential stimulator system (Medoc Advanced Medical Systems, Israel) was used to deliver heat pain stimuli. Stimuli were applied for 2 s each on the medial side of the lower right leg. The location of the heat probe was adjusted between applications to reduce sensitization. Temperatures were calibrated for every subject. For the familiarity and calibration phase, we first performed one ascending sequence. In the ascending sequence, the temperature started from 38 °C with a step of 1 °C and ended at 50 °C or at the temperature the subject could tolerate. Pain ratings were measured in accordance with Gracely Sensory Scales (0–20) (Chapman et al., 1985; Gracely et al., 1978). Three temperatures that each subject rated as 5–6 (low pain), 10–11 (moderate pain), and 14–15 (high pain) were selected. After selecting three temperatures, we then applied 3 random pain sequences (three trials for low, moderate, and high pain respectively, a total of 9 trials in each sequence) and 3 identical pain sequences (six trials for low or moderate or high pain in each sequence), to test the validity of calibrated temperatures.

2.3.   Experimental design

The experiment consisted of a conditioning phase and a test phase conducted on the same day (Fig. 1 A).

2.3.1.   Conditioning phase—Subjects underwent two runs of direct conditioning and two runs of indirect conditioning in a randomized order. Each run contained 20 trials. Visual cues consisted of forward-facing, emotionally neutral male faces obtained from the Karolinska Directed Emotional Faces (KDEF) set (Goeleven et al., 2008). Images were displayed with Presentation software (Version 16.3, www.neurobs.com), and the assignment of images to a given condition was counterbalanced across subjects.

In direct conditioning, subjects were told that they would be presented with faces and pain ratings on a screen, and each face was paired with a pain stimulus (i.e., they were not told that they would receive high or low pain stimuli) on their leg. A heat pain stimulus was applied to the leg 1 s after a cue was presented on the screen. Two cues (i.e., male faces, Fig. 1 A) were presented in a random order, 10 times per cue. One cue was presented with a high pain stimulus and the other with a low pain stimulus. Subjects rated each stimulus on a 0–10 visual analogue scale (VAS; 0 being no pain and 10 being the worst pain possible). Two different pain rating scales were used in the calibration and conditioning/test phases (0–20 Gracely scale vs. 0–10 VAS). This aimed to ensure that subjects focused on their immediate pain experience during the test phase rather than any recollections of the calibration phase.

In indirect conditioning, subjects were shown a video of a model participant undergoing direct conditioning rather than receiving pain themselves. The model appeared in front of a computer with a heat probe on their leg. Subjects saw the cue (i.e., male faces, Fig. 1 A) that was presented to the model, the model's facial reaction in response to the cue, and the model's pain rating. The facial pain depictions were obtained from a research assistant in the lab showing a painful or non-painful expression without receiving real pain stimuli. The cue, facial pain expression, and pain rating in one conditioning trial were paired to link the cue and expectation of pain. Two new cues were presented in a random order, 10 times per cue. One cue was paired with high pain and the other with low pain. The model's ratings average pain ratings were 2.0 ± 0.4 for low pain and 8.1 ± 0.4 for high pain.

Please refer to Fig. 1 A for the timings of a standard conditioning trial. In direct conditioning, a cue was presented for 500 ms, and subjects received heat pain 1000 ms after the cue disappeared. The target temperature was sustained for 2000 ms, and subjects rated their pain intensity 5000 ms after the heat stimulus ended. Subjects were allotted 5000 ms to rate their pain. In indirect conditioning, the model's initial expression was shown for 2000 ms. After 4000–7000 ms (pseudorandomized), subjects saw a cue for 500 ms. After 1000 ms, during which the model presumably received a heat pain stimulus, they saw the model's reaction (painful or not painful) to the stimulus for 2000 ms. Subjects observed how the model rated their pain intensity 5000 ms after the pain stimulus, and the rating procedure lasted 5000 ms. The timings from cue onset to pain rating for both direct and indirect conditioning were the same in order to control for the duration of learning the association between cue and pain.

Following the conditioning phase, subjects were presented with an array of 9 faces and asked to identify the 4 learned cues. Further, they had to indicate whether the cue was direct or indirect and high pain or low pain. Subjects who correctly identified these 4 cues immediately proceeded to the test phase (two were not able to identify). The time gap between the conditioning phase and test phase was around 5 mins.

2.3.2.   Test phase—During the test phase, subjects were told that they would be presented with the four familiar cues and one unfamiliar cue. They were also informed that some cues would be fully visible (supraliminal, 500 ms) while others would appear only briefly and would be followed by a masking image (subliminal, 33 ms cue + 467 ms mask) such that the cue may be unrecognizable. An identical moderate pain stimulus was delivered with each cue to test the conditioning effect. The test phase took place in three runs, with each run consisting of 60 trials for each of 10 different cues (5 supraliminal and 5 subliminal). Cues were presented 6 times in each run (18 times total). For each cue, subjects were prompted to rate their pain sensation in 1/3 of the total trials for that cue (6 out of 18 trials; to reduce the length of experiment and reduce fatigue of participants and to avoid recollection of rating of the former trial). We thus collected six pain ratings for each of the 10 cues (supraliminal and subliminal presentations of direct high and low, indirect high and low, and neutral cues) for each subject. Please refer to Fig. 1 A for the timings of a standard test trial.

Following the test phase, subjects were presented with cues from the experiment in addition to novel cues, presented supraliminally and subliminally. They were asked whether or not they recognized these cues to ensure that recognition of the subliminal stimuli was at chance level.

2.4.   MEG and structural MRI acquisition

MEG data were recorded during the test phase for each subject. The MEG data were acquired inside a magnetically shielded room using a whole-head Elekta Neuromag VectorView system (Helsinki, Finland) composed of 306 sensors arranged in 102 triplets of two orthogonal planar gradiometers and one magnetometer. The data were sampled at 1000 Hz after 300 Hz anti-aliasing low-pass filtering. T1-weighted, high-resolution magnetization prepared rapid acquisition gradient-echo (MPRAGE) structural images were collected on a 3T Siemens Trio whole-body MRI scanner (Siemens Medical Systems, Erlangen, Germany) using a 32-channel head coil.

2.5.   MEG preprocessing and source analysis

Maxfilter software (Elekta Neuromag, Helsinki, Finland) was applied on the acquired MEG data for head movements compensation and denoising using spatiotemporal filters (Taulu and Simola, 2006). Brain-storm software was used to extract epochs from 200 ms before cue onset to 1500 ms after cue onset and to preprocess the data. We removed the baseline mean of each sensor (−200 to 0 ms) and lowpass filtered the data at 100 Hz. Epochs with peak-to-peak magnitude greater than 10,000 fT were excluded from further analyses (< 1% of epochs per subject). For the subsequent multivariate pattern analysis, the data of each sensor were divided by the standard deviation of the pre-stimulus baseline signal of that sensor.

Source activation maps were computed on subject-specific cortical surfaces derived from Freesurfer (https://surfer.nmr.mgh.harvard.edu/). The forward model was calculated using an overlapping spheres model (Huang et al., 1999). MEG signals were then mapped on the cortex using a dynamic statistical parametric mapping approach (dSPM) (Dale et al., 2000).

2.6. MEG multivariate pattern analysis

For each time point in the peri-stimulus MEG signal, from −200 ms to 1500 ms (1 ms resolution) with respect to cue onset, we extracted pattern vectors by concatenating the 306 MEG sensor measurements into 306-dimensional vectors, resulting in 18 pattern vectors for each cue. We then used a linear support vector machine (SVM) classifier (LIBSVM library) (Chang and Lin, 2011) to classify pairwise between conditions (e.g., 18 trials of direct conditioned, consciously perceived high pain cues vs. 18 trials of direct conditioned, consciously perceived low pain cues) with five-fold cross-validation (Fig. 2 A and B). The pairwise classification was repeated 100 times with random assignments of trials into five folds, and the resulting decoding accuracies were averaged over repetitions. The results of the classification (percentage decoding accuracy, 50% chance level) were stored in an 8×8 symmetric decoding matrix (each cell in the matrix indicating the decoding accuracy with which the classifier distinguished between two face cues) per time point and subject (Fig. 2 C). We further partitioned the decoding matrix into segments for pairs of within consciousness and unconsciousness since direct comparisons between consciously and unconsciously perceived cues would be driven by the effect of the masking image.

In addition to decoding high and low pain cues, we used the same temporal decoding approach to classify intra-subject pain levels (high pain vs. low pain) across trials, despite the fact that subjects received the same moderate pain stimuli for all trials. This analysis enabled us to understand how expectancy-modulated anticipatory MEG brain activity can predict subsequent variation of subjective pain perception. Given that we only required subjects to rate 1/3 of all trials (i.e., 30 trials for consciously and unconsciously perceived cues respectively), the prediction was performed by sorting trials according to subjects' pain ratings and equally dividing them into two classes (i.e., high pain and low pain). To avoid the identical pain ratings when splitting trials into two groups (i.e., the 15th and nearby trials after sorting) and to increase prediction power, we only selected the 10 trials (i.e., top 1/3) with the highest pain ratings and the 10 trials (i.e., bottom 1/3) with the lowest pain ratings to be split into two groups. We then performed binary classification using the anticipatory MEG measurements after consciously and unconsciously perceived cues, respectively.

We also generalized the decoding procedure across time by training the SVM classifier at a given time point *t* and testing across all other time points (Cichy et al., 2014; Pantazis et al., 2018). Intuitively, if representations are stable over time, the classifier should successfully discriminate signals not only at the trained time *t*, but also over extended periods of time that share the same neural representation of expectancy. This temporal generalization analysis was repeated for every pair of cues, and the results were averaged across conditions (e.g., high cue vs. low cue) and subjects, yielding 2-dimensional temporal generalization matrices with the x-axis denoting training time and y-axis denoting testing time.

2.7. Identifying spatiotemporal dynamics for decoding

The time-resolved classification yielded vectors of classification weights for 306 sensors at each time point for each subject. We then transformed these weights into patterns using Haufe's method (Haufe et al., 2014). To provide an accurate understanding of the spatial and temporal origins of the decoding signals, we mapped these sensor-level patterns to subject-specific cortical source estimates using dSPM (Dale et al., 2000). We were particularly interested in several time of interests (TOIs) based on the results of temporal decoding (see Fig. 4 A and B for details): (1) during cue presentation (0–500 ms), we selected the TOIs as the onset of significance and two peaks in the time course of decoding accuracy; (2) after cue presentation (500–1000 ms), we selected every 100 ms in the time course of decoding accuracy; and (3) the offset of significant in the time course of decoding accuracy. We then performed statistical testing at each TOI across subjects to identify spatiotemporal clusters with significant contributions in decoding high and low pain cues.

After identifying spatiotemporal clusters with significant contribution, we extracted the brain response in each cluster and correlated with the corresponding single-trial perceived pain intensities using Pearson's correlation analysis to investigate their relationship in the pain anticipation period (Atlas et al., 2010). To minimize the influence of individual differences (Hu and Iannetti, 2019; Tu et al., 2019), single-trial pain intensities were normalized within each subject by subtracting their mean and dividing by their SD before performing the correlation analysis. The obtained correlation coefficients were Fisher's z-transformed, and the resulting z values were compared against 0 using a one-sample *t*-test and p values were corrected for multiple comparisons using FDR.

2.8. Mediation analysis

We performed bootstrapped mediation analyses to assess the mediatory role of anticipatory brain responses (see Fig. 5 for details) on the relationship between cue-based expectancy and pain perception, using the PROCESS macro (version 2.16.3) in SPSS (IBM, version 22.0.0) with 1000 bootstrap samples. This analysis identified 95% confidence intervals for model components. With categorical values as the independent variable (coded as 1, 0, and −1 for high, neutral, and low cues, respectively) (Hayes and Preacher, 2014) and perceived pain intensities (i.e., individuals' pain ratings for high, neutral, and low cues, respectively) as the outcome, we tested whether brain responses showing significant correlations with pain intensities mediated the relationship between cue-based expectancy and pain perception. A mediation was considered significant when bootstrapped upper and lower 95% confidence intervals did not include zero (Hayes and Preacher, 2014).

2.9. Statistical considerations

For the statistical assessment of behavioral results, we first performed a three-way repeated-measures analysis of variance (ANOVA) compare the subjective pain ratings to identical moderate heat pain stimuli, with factors of cue (high vs. neutral vs. low), conditioning type (direct vs. indirect), and awareness (conscious vs unconscious). When the main effect was significant, post-hoc paired-sample *t*-test with Tukey correction was applied. We also compared the magnitudes of placebo analgesia (i.e., pain ratings following neutral cues minus those following low pain cues) and nocebo hyperalgesia (i.e., pain ratings following

high pain cues minus those following neutral cues) using a three-way repeated-measures ANOVA, with factors of modulation type (placebo vs. nocebo), conditioning type (direct vs. indirect), and awareness (conscious vs. unconscious).

For the statistical assessment of classification time series and temporal generalization matrices, we performed nonparametric permutation-based cluster-size inference (Maris and Oostenveld, 2007). The null hypothesis was equal to 50% chance level for decoding results. In all cases, we could permute the labels (high or low cue) of the MEG data, which was equivalent to a sign permutation test that randomly multiplied subject responses by $+ 1$ or -1. We used 1000 permutations; 0.05 cluster defining threshold and 0.05 cluster threshold were used for time series, and 0.001 cluster defining threshold and 0.05 cluster threshold were used for temporal generalization maps (we used a stringent threshold for temporal generalization since it had more multiple comparisons).

For the statistical assessment of differences in latencies and peak accuracies between decoding consciously and unconsciously perceived cues (i.e., decoding consciously perceived cues reached significance earlier, had higher accuracies, and maintained significance longer), we performed 1000 bootstrap tests (with replacement) over 21 subjects and performed decoding on bootstrapped samples. The resulting latencies (i.e., the first and last time points above significance; 1000 samples) and accuracies were compared using a paired t-test.

For the identification of spatiotemporal dynamics in the source space, we compared classification patterns against zero using a one-sample t-test across 21 subjects, resulting in a t-value map at each time point. The t-value maps were set at a threshold of $p < 0.001$ uncorrected and $p < 0.05$ false discovery rate (FDR) corrected at the cluster level.

3. Results

3.1. Behavioral and brain responses after pain stimuli

During the conditioning phase, four different cues were associated with a high or low level of directly or indirectly perceived heat pain. Pain ratings between the low and high pain stimuli were significantly different ($t_{20} = 33.8$, $p < 0.001$; paired-sample t-test): low pain stimuli elicited an average rating of 1.6 ± 0.5 (mean $\pm$ SE) and high pain stimuli elicited an average rating of 7.4 ± 0.7.

During the test phase (Fig. 1 B), ANOVA results indicated a significant main effect of cue ($F_{2,40} = 17.89$, $p < 0.001$, $\eta^2 = 0.25$), and non-significant main effects of conditioning type ($F_{1,20} = 0.38$, $p = 0.54$, $\eta^2 = 0.002$) and awareness ($F_{1,20} = 0.11$, $p = 0.74$, $\eta^2 = 0.0002$) on subjective pain ratings. Post-hoc analysis showed that pain ratings for high pain cues (3.93 ± 0.38) were significantly higher than pain ratings for neutral (3.40 ± 0.35; $t_{20} = 4.2$, $p < 0.001$, Cohen's $d = 0.44$) and low cues (3.19 ± 0.34; $t_{20} = 6.2$, $p < 0.001$, Cohen's $d = 1.36$), while pain ratings for low cue were marginal significantly lower than pain ratings for neutral cue ($t_{20} = 2.0$, $p = 0.05$, Cohen's $d = 0.44$).

We also observed a significant effect of interaction between cue and awareness ($F_{2,40} = 10.18$, $p < 0.001$, $\eta^2 = 0.11$), demonstrating that expectancy effects were stronger after consciously perceived cues compared to unconscious perceived ones (i.e., pain ratings after high cues were higher, while pain ratings after low cues were lower in trials with consciously perceived cues than in trials with unconsciously perceived cues; high conscious vs. high unconscious: $t_{20} = 4.6$, $p < 0.001$, Cohen's $d = 1.0$; low conscious vs. low unconscious: $t_{20} = 4.9$, $p < 0.001$, Cohen's $d = 1.1$). Pairwise comparisons between low and high cues were significant in the direct conscious ($t_{20} = 4.2$, $p < 0.001$, Cohen's $d = 0.92$), indirect conscious ($t_{20} = 5.3$, $p < 0.001$, Cohen's $d = 1.16$), and direct unconscious trials ($t_{20} = 2.3$, $p = 0.031$, Cohen's $d = 0.47$), but not in the indirect unconscious trials ($t_{20} = 1.6$, $p = 0.14$, Cohen's $d = 0.31$).

We then compared pain ratings for conditioned cues (high and low) to neutral cues and found significant placebo analgesia and nocebo hyperalgesia in conscious trials (direct placebo: $t_{20} = 1.9$, $p = 0.033$, Cohen's $d = 0.42$; direct nocebo: $t_{20} = 4.1$, $p < 0.001$, Cohen's $d = 0.91$; indirect placebo: $t_{20} = 3.4$, $p = 0.001$, Cohen's $d = 0.74$; indirect nocebo: $t_{20} = 4.3$, $p < 0.001$, Cohen's $d = 0.93$). However, we only found directly conditioned significant nocebo hyperalgesia in nonconscious trials ($t_{20} = 1.9$, $p = 0.034$, Cohen's $d = 0.42$). ANOVA results showed significant main effects of modulation type ($F_{1,20} = 7.79$, $p = 0.011$, $\eta^2 = 0.06$) and awareness ($F_{1,20} = 14.1$, $p < 0.001$, $\eta^2 = 0.13$), but not conditioning type ($F_{1,20} = 0.38$, $p = 0.54$, $\eta^2 = 0.001$) nor any of their interactions on the magnitudes of placebo and nocebo effects. Post-hoc analyses showed that nocebo effects (0.53 ± 0.18) were significantly higher than placebo effects (0.21 ± 0.14; $t_{20} = 1.9$, $p = 0.011$, Cohen's $d = 0.61$), and effects in conscious trials were significantly higher than nonconscious trials ($t_{20} = 3.8$, $p = 0.001$, Cohen's $d = 0.82$).

The group-level waveforms of the pain-evoked brain responses to identical moderate heat pain stimuli at a representative MEG sensor (central somatosensory cortex) following different types of face cues (i.e., high, low, and neutral expectancy) are detailed in the Supplementary Figure S1. In the present study, we focus on the brain responses and mechanisms during anticipation of pain other than during experience of pain.

3.2. Brain responses after predictive cues

We recorded MEG data while participants viewed five face cues either consciously or unconsciously during the test phase. Fig. 3 shows the group-level waveforms of the visual evoked brain responses at a representative MEG sensor (right temporal lobe) elicited by five different face cues. The topographies and magnitudes corresponding to the three prominent deflections are included in the figure and labeled according to their approximate peak latencies: M120, M170, and M250. We used a two-way repeated-measures ANOVA with factors of cues (high vs. low) and conditioning type (direct vs. indirect) to assess the differences in amplitudes and latencies of these three major peaks for consciously and unconsciously perceived cues, respectively. Please note that we did not compare the consciously perceived cues to the unconsciously perceived cues to avoid the confounding effects introduced by masking in the subliminal cues.

We found a significant effect of cue ($F_{1,20} = 4.9$, $p = 0.04$) on the magnitudes of M120 after unconsciously perceived face cues, and we did not find any significant effects of conditioning type on the three deflections. Since direct and indirect conditionings had similar effects on behaviors and brain responses in the present study and our previous studies (Egorova et al., 2015; Tu et al., 2018), we combined the trials with directly and indirectly conditioned face cues and compared the magnitudes and latencies of the three deflections between low and high pain cues (Fig. 3, lower panel). Although not significant, M170 had a trend of higher magnitudes after high pain cues for both consciously ($p = 0.07$) and unconsciously ($p = 0.08$) perceived trials.

3.3. Time course of decoding high and low pain cues

To determine the time course of expectancy processing between cue onset and pain stimulus onset, we performed a time-resolved multivariate pattern analysis on the MEG signals recorded while subjects perceived supraliminal and subliminal face cues. Figs. 4 A and B show the time courses of neural decoding accuracy for consciously and unconsciously perceived face cues with wide band (0 – 100 Hz) MEG data from all sensors. The time course of the decoding of high and low pain cues was obtained by averaging the time courses of the four between-expectation pairs in the consciously perceived and unconsciously perceived trials respectively (i.e., direct high vs. direct low, direct high vs. indirect low, indirect high vs. direct low, indirect high vs. indirect low; see asterisks in the figure). Consciously perceived cues (high vs. low) could be discriminated in a cluster that began at 148 ms (decoding first reached significance), reached a peak at 249 ms (70.0% mean decoding accuracy), and remained significantly above chance until 1095 ms after cue onset (cluster-corrected sign permutation test; cluster-defining threshold $p < 0.05$, corrected significance level $p < 0.05$).

Unconsciously perceived cues could be discriminated in a cluster that began at 151 ms (decoding first reached significance), reached a peak at 283 ms (66.7% mean decoding accuracy), and remained significantly above chance until 1041 ms after cue onset (cluster-corrected sign permutation test; cluster-defining threshold $p < 0.05$, corrected significance level $p < 0.05$). Direct comparisons of two time courses showed that decoding consciously perceived cues (1) reached significance earlier (consciously perceived cues: 95% confidence interval [CI], 146 to 150 ms; unconsciously perceived cues: 95% CI, 150 to 157 ms; $p < 0.001$, bootstrap testing); (2) was around 2% higher in peak decoding accuracy ($p < 0.001$, paired-sample t-test); (3) had significantly higher decoding accuracy between 205 ms and 261 ms (cluster-defining threshold $p < 0.05$, corrected significance level $p < 0.05$); and (4) maintained significance for around 50 ms longer (consciously perceived cues: 95% CI, 1093 to 1097 ms; unconsciously perceived cues: 95% CI, 1039 to 1044 ms; $p < 0.001$, bootstrap testing).

We also performed similar analyses using MEG data from different frequency bands and observed that the delta band (1 – 3 Hz) and theta band (4 – 7 Hz) played a major role in decoding high and low pain cues (Supplementary Fig. S2). This finding is compatible with previous studies indicating that percepts tend to be locked to a theta or high delta rhythm (Melloni et al., 2007; Nakatani et al., 2014; Sitt et al., 2014). It is possible that the MEG

decoding reflects viewing different faces independent of the conditioned expectancy. However, this account seems unlikely here since (1) the significance in decoding face perception can reach significance as fast as about 50 ms (Dobs et al., 2019), and (2) the face cues with the same expectation level (e.g., direct high vs. indirect high) could not be distinguished by the MEG data (Supplementary Fig. S3).

To explore the possible effect of conditioning type on time-resolved decoding, we demonstrated the time courses of decoding (1) direct high vs. direct low and (2) indirect high vs. indirect low for consciously and unconsciously perceived cues, respectively (Supplementary Fig. S4). Results showed that the method of conditioning did not significantly affect decoding performance (i.e., time windows with decoding significance, decoding accuracies) for both conscious and unconscious trials. Together with our previous study, which showed that direct and indirect conditioning had both shared and distinct modulatory effects on brain networks before and after conditioning (Tu et al., 2018), we believe that once expectations have been learned and stored through conditioning, the resolving process may be similar for direct and indirectly perceived expectations.

In addition, we also tested the time-resolved decoding between conditioned cues and neutral cue (Supplementary Figure S4). For consciously perceived cues, the decoding between high and neutral cues was not significantly different than that between low and neutral cues. However, the decoding accuracies were significantly higher when discriminating unconsciously perceived high and neutral cues than when discriminating unconsciously perceived low and neutral cues. This finding is consistent with behavioral placebo/nocebo effects, showing that the discrimination of unconsciously perceived high and low cues may be driven by the difference of high and neutral cues.

3.4. Temporal generalization of decoding high and low pain cues

To test how persistent the neural responses are in distinguishing face cues, and thereby to shed light on the temporal organization of expectancy-processing stages (King and Dehaene, 2014), we performed a temporal generalization analysis (Cichy et al., 2014; Pantazis et al., 2018). Fig. 4 C and D show the 2-dimensional decoding matrices with the x-axis indexed by training time and the y-axis indexed by testing time for consciously and unconsciously perceived cues, respectively.

Overall, the classifier generalized best to neighboring time points and performed poorly for distant time points. This is illustrated by the highest decoding accuracy along the diagonal and the drop in accuracy away from the diagonal in Fig. 4 C and D. We found two main stages for decoding consciously perceived cues (Fig. 4 C). First, the significance map (cluster-corrected sign permutation test, cluster-defining threshold $p < 0.001$, corrected significance level $p < 0.05$) formed a square pattern, which indicates a sustained neural activity for decoding, from ~150 ms to the offset of cue presentation at 500 ms, and extended to ~600 ms. Second, the significance map switched to a diagonal pattern with a lack of generalization, which suggests transient neural activities and continuous processing of expectancy after cue presentation, from ~600 to ~1100 ms. In contrast, the significance map of decoding unconsciously cues (Fig. 4 D) showed an early diagonal pattern (from 160 ms to 250 ms), then broadened considerably to a sustained pattern (from 250 ms to 600 ms),

and finally switched back to a diagonal pattern (from 600 ms to 1000 ms). The temporal generalization results for different frequency bands are provided in Supplementary Fig. S6.

Taken together, decoding consciously and unconsciously perceived low and high pain cues had both shared and distinct neutral dynamics. The neural patterns related to decoding consciously perceived cues were predominately sustained and generalized well during cue presentation but lacked generalization after the cue. In contrast, the patterns related to decoding unconsciously perceived expectancy changed rapidly during the early processing of a face cue and showed a shorter sustained period of being above chance level after the cue.

3.5. Spatiotemporal patterns of decoding high and low pain cues

Fig. 4 E shows spatiotemporal patterns that significantly contributed to the decoding of consciously perceived high and low pain cues. During cue presentation, we selected three key time points based on the time course of decoding accuracy in Fig. 4 A: the onset of significance (t_{1c} = 148 ms) and two peaks (t_{2c} = 249 and t_{3c} = 385 ms). We observed multiple significant clusters (for which the brain responses were larger after a low cue than a high cue; shown in blue in Fig. 4 E) during early visual processing (t_{1c} and t_{2c}), including the primary visual cortex (i.e., calcarine sulcus and cuneus), inferior temporal gyrus, fusiform gyrus, precuneus, and lingual gyrus. The significant clusters were found in the primary visual cortex as well as the thalamus, paracentral lobule (ParaCL), and middle cingulate cortex in the late stage (t_{3c}). After cue presentation (600 – 1000 ms), we observed a consistent distribution of significant patterns (for which the brain responses were larger after a high cue than after a low cue; shown in red in Fig. 4 E) in the dorsal medial prefrontal cortex (dMPFC). This pattern was also observed in the last time point when the decoding was significant (t_{4c} = 1095 ms), with another significant cluster with positive responses in the dorsal anterior cingulate cortex (dACC).

Fig. 4 F shows the spatiotemporal patterns for decoding unconsciously perceived high and low pain cues. During cue presentation, we again selected three time points according to Fig. 4 B (t_{1u} = 151 ms, t_{2u} = 283 ms, t_{3u} = 434 ms). We found similar patterns as in the case of consciously perceived trials in the primary visual cortex and precuneus in the early stage (t_{1u} and t_{2u}) and ParaCL in the late stage (t_{3u}), as well as distinct clusters in the right temporoparietal junction (rTPJ) and middle temporal gyrus (MTG) at t_{2u}. Interestingly, we also found significant contributions that were larger after a high cue than after a low cue from the dMPFC after unconscious cue presentation and from the dACC at the last time point with significance in decoding (t_{4u} = 1041 ms).

3.6. Brain responses mediate cue-based expectancy of pain

To associate the expectancy-modulated brain responses with pain perception, we correlated the spatiotemporal neural activities identified in Fig. 4 E and F with corresponding self-reported pain intensities at single-trial level for each subject. After consciously perceived cues (Fig. 5 A), we only found that brain responses in the dACC at t_{4c} (1095 ms) were significantly positively correlated with pain intensities (r = 0.26 ± 0.19, mean ± SD; $p <$ 0.001), indicating that a stronger brain response in the dACC during the pain anticipation

period was associated with a higher perceived pain intensity during the pain experience period. To assess the mediatory role of these spatiotemporal dynamics on the relationship between cue and pain perception, we performed a bootstrapped mediation analysis and found that the dACC at t_{4c} significantly mediated cue-based expectancy of pain intensities (path $a = 0.24$, $p < 0.05$; path $b = 0.40$, $p < 0.01$; direct effect = 0.58, $p < 0.001$; indirect effect = 0.09, 95% CI: 0.0005 – 0.2354; Fig. 5 B). This result suggests that individuals who had larger cue effects on the dACC also had larger cue effects on pain.

After unconsciously perceived cues (Fig. 5 C), we also found similar results, i.e., we only found that brain responses at the dACC at t_{4u} (1037 ms) were positively correlated with pain intensities ($r = 0.14 \pm 0.23$, $p = 0.01$). We did not perform mediation analysis since the total effect between unconsciously perceived cues and pain intensities was not significant.

As shown in Fig. 5 D and E, the pain levels could be predicted after ~170 ms for both consciously and unconsciously perceived cues and maintained predictability prior to the pain stimulus (up to 1476 ms) for the consciously perceived cues (cluster-corrected sign permutation test, cluster-defining threshold $p < 0.05$, corrected significance level $p < 0.05$) but not for the unconsciously perceived cues (up to 1063 ms).

4. Discussion

In this study, we combined a visual conditioning paradigm and MEG to investigate how expectations of pain elicited by consciously and unconsciously perceived cues unfold over time. First, we found that high and low pain cues could be accurately decoded from MEG, whether or not the visual cue was perceived with consciousness but differed in time. Second, neural dynamics associated with decoding consciously perceived cues were predominately sustained during cue presentation but transient after cue presentation. In contrast, decoding unconsciously perceived cues had rapidly changing patterns of neural activity during the early processing of cues but later followed similar generalization patterns as those in the consciously perceived cues. Third, source localization traced brain regions underlying the decoding of high and low pain cues. While decoding consciously perceived cues benefited from a series of additional time-restricted brain regions during cue presentation, the decoding relied on the dMPFC and dACC after cue presentation for both consciously and unconsciously perceived cues. Finally, the within-subject conditioned pain-related responses could be predicted by the anticipatory MEG after 170 ms of cue onset and maintained predictability prior to the pain stimulus for the consciously perceived trials only.

4.1. Cue-based expectation modulates pain perception

Using a conditioning model and cue-based manipulations of stimulus expectancy, previous studies have revealed that short-term expectations that vary as a function of cue could be conditioned by both self-experience (Atlas et al., 2010; Shih et al., 2019; Tu et al., 2020) and social observation (Colloca and Benedetti, 2009; Hunter et al., 2014; Schenk and Colloca, 2020; Tu et al., 2018). These expectations have strong effects on pain perception and pain-evoked responses. Consistent with these studies, our results showed that cue-based expectancy modulated perceived intensity to pain. In addition, as supported by previous studies (Jensen et al., 2015, 2012), we found that perceived pain intensities following

unconsciously perceived high pain cues were significantly higher than those following low pain cues ($p = 0.03$). These findings could thereby translate the investigation of unconscious effects to the clinical realm by suggesting that health-related responses can be triggered by cues that are not consciously perceived in a variety of medical problems (e.g., pain, asthma, depression, and irritable bowel syndrome) (Kaptchuk et al., 2008; Moncrieff and Kirsch, 2005; Wechsler et al., 2011). It is worth mentioning that we were not able to verify whether expectations were being processed consciously or unconsciously. In case of over-interpretation, we termed our findings as expectations elicited by consciously and unconsciously perceived cues.

Although behavioral results suggest that both consciously and unconsciously perceived cues can modulate subsequent pain perception, the underlying neural mechanisms remain poorly understood. Previous neuroimaging studies have focused on investigating the expectancy-modulated brain responses during pain (Atlas et al., 2010; Freeman et al., 2015; Wager et al., 2007). One study by Wager and colleagues provided evidence that the prefrontal cortices (e.g., dorsal medial prefrontal cortex, orbitofrontal cortex) have been involved in the processing of conditioned expectancy during pain anticipation (Wager et al., 2004). A later study showed that cue-evoked anticipatory activity in the medial orbitofrontal cortex and ventral striatum mediated cue effects on pain-evoked brain responses (Atlas et al., 2010). Our work goes beyond previous findings in two important respects. First, we provided direct evidence of how cue-based expectancy resolves over time. Second, we showed distinct spatiotemporal dynamics for expectations elicited by consciously and unconsciously perceived cues. In the following, we will discuss these in more detail.

4.2. Decoding face cue-based expectancy over time

While a few prior studies have investigated the time course of face perception using MEG and machine learning techniques (Cichy et al., 2014; Dobs et al., 2019; Vida et al., 2017), they have mainly focused on the decoding of different facial dimensions (e.g., identity, age, gender). Our study, for the first time, extended brain decoding to the information (i.e., expectancy) encoded in face cues. Decoding expectation requires additional brain resources and is inevitably slower than decoding facial dimensions. For example, one recent study showed that individual faces could be discriminated by visual representations as early as ~50 ms, and while different facial dimensions follow coarse-to-fine processing (Besson et al., 2017), they were significantly decoded no later than 100 ms after stimulus onset (Dobs et al., 2019). Therefore, our results suggest that face cue-based expectancy could have been decoded (~150 ms) after the basic facial dimensions were identified. On the other hand, our decoding remained significantly above chance until ~1100 after cue onset. Although previous studies have shown that brain signals prior to pain stimuli would modulate subsequent pain perception (Tu et al., 2016), we found that the expectancy was not decodable within 1100 –, 1500 ms after cue onset (i.e., –400 – 0 ms before pain stimulus onset). This may be due to the fact that, in this time window, expectancy could not be detected by sensor-level MEG or stored as another format (e.g., memory) in the brain.

The temporal generalization matrices, appearing as a short diagonal pattern at the initial decoding stage (~150 – 250 ms), and our source analyses suggest that a fast sequence of

neural responses propagated from the primary visual cortex to visual association regions. This is similar to the results of a number of previous studies (Cichy et al., 2014; King and Dehaene, 2014; Salti et al., 2015). The matrices then broadened considerably to a squared pattern during the cue presentation, indicating sustained neural activity in parietal and sensorimotor areas that are generalized well for decoding (King and Dehaene, 2014). Following the offset of the cue, the temporal generalization matrices switched back to a diagonal pattern. This suggests a sequence of neural activities reflecting the hierarchical processing and evaluation of expectancy (King and Dehaene, 2014). In this stage, the neural activity finally reached the frontal cortices (primarily the dMPFC) and prepared the 'brain state' for the upcoming pain stimulus (Boly et al., 2007; Buzsaki, 2006; Tu et al., 2016).

4.3. Neural dynamics for expectations elicited by consciously and unconsciously perceived cues

The human brain can process sensory information before it reaches conscious awareness (Dehaene and Changeux, 2011; Pessiglione et al., 2008, 2007). Therefore, conditioned expectancy elicited by the subliminally-presented cues can mediate unconscious effects on pain perception. Our previous study using fMRI revealed that positive expectancy of pain was associated with increased activation of the OFC, while negative expectancy of pain was associated with increased activation of the thalamus, amygdala, and hippocampus during the experience of pain (Jensen et al., 2015). The present study, notably, presented both distinct and shared neural dynamics at the milliseconds level for the processing of expectations elicited by consciously and unconsciously perceived cues during pain anticipation.

First, we noticed that decoding unconsciously perceived high and low pain cues reached significance more slowly, had lower decoding accuracy, and decayed faster than decoding consciously perceived cues. This finding is consistent with previous studies showing that both decoding and behavioral performance are typically higher for conscious percept given the depth of processing (Dehaene and Changeux, 2011; King et al., 2016; Lau and Passingham, 2006; Salti et al., 2015), and suggests that the human brain may need more time to extract expectancy from unconsciously perceived cues, may have weaker effect for the discrimination of high and low pain expectations, and shorter time to maintain the information.

Second, we found that different neural processes may follow consciously and unconsciously perceived cues, especially during the presentation of the stimuli. Similar to the findings in Salti et al., 2015, although the processing of cue-based expectation followed a hierarchical network – that is, neural dynamics moved from the primary visual cortex to higher visual regions and finally reached the parietal cortices during cue onset – we found that the processing of consciously perceived cues recruited additional brain regions (e.g., fusiform, thalamus, middle cingulate cortex), each restricted in time. Given that conscious perception produced more extensive and structured brain activity for processing expectation, it may explain why conscious effects were stronger than unconscious effects for both decoding performance and behavior responses.

Third, after cue presentation, we found that the processing of consciously and unconsciously perceived cues may follow a similar pattern of neural dynamics in the dMFPC. The dMFPC

is an important node in the neural circuit which subserves the perception of negative emotional cues and the arousal components of feeling negative emotions (Kober et al., 2008). Although the spatiotemporal patterns of the decoding activities were consistently observed in dMPFC after 600 ms, the expectation were hierarchically but not sustainably processed (as reflected by the lack of temporal generalization). Neural dynamics finally reached the dACC to mediate the conscious expectancy effects on subsequent pain perception, which is compatible with a previous fMRI study showing that the dACC is a mediator of predictive cue effects on perceived pain (Atlas et al., 2010). Although we did not find significant mediation for unconscious effects, which may be due to the fact that the total unconscious effect was not significant, neural activity in the dACC was also correlated with perceived pain. In addition, these results suggest that expectations could modulate neural dynamics in the salience network (e.g., dACC) and the default mode network (e.g., dMPFC), and consequently modulate pain perception. The association between expectation fluctuation and pain variability may also be encoded in the dynamic pain connectome which may reflect pain variability encoded in the neural dynamics of brain networks including the salience network, default mode network, and antinociceptive network (Bosma et al., 2018; Kim et al., 2020; Kucyi and Davis, 2015).

4.4. Limitation and future direction

First, the heat pain stimulator produced large artifacts that degraded the quality of the MEG data after pain stimuli. Future studies using other stimulators (e.g., laser, electric) will be useful in uncovering causal relationships between expectation, neural dynamics, and pain. Second, we used an SVM classifier to discriminate low and high pain cue conditions. The cues were associated with expectations towards different levels of pain, but we could not completely rule out the possibility of other factors (e.g., emotion) contributing to the discrimination. Third, we did not record expectation scores during the experiment and therefore we were not able to track trial-by-trial fluctuations of expectation of pain and directly associate expectation scores with neural dynamics. Future study will include expectation assessment during pain expectation to investigate the dynamic nature of expectations. Fourth, although we were able to statistically compare the time courses of decoding accuracies, due to the design of our experiment (using the masking image to induce subliminally perceived expectation), we were not able to perform decoding across conscious and unconscious cues since the effect would be driven by the masking image and thus were not able to directly assess the differences of spatiotemporal profiles between conscious and unconscious cues. This limited us to quantitatively assess the differences of consciously and unconsciously decoding processes.

5. Conclusion

The present study provides insight into how expectations of pain elicited by consciously and unconsciously perceived vidual cues unfold over time. Understanding the temporal infrastructure of conscious and unconscious processes in placebo and nocebo effects may enhance clinical care by demonstrating the impact of expectation cues conveyed during therapy.

Supplementary Material

Refer to Web version on PubMed Central for supplementary material.
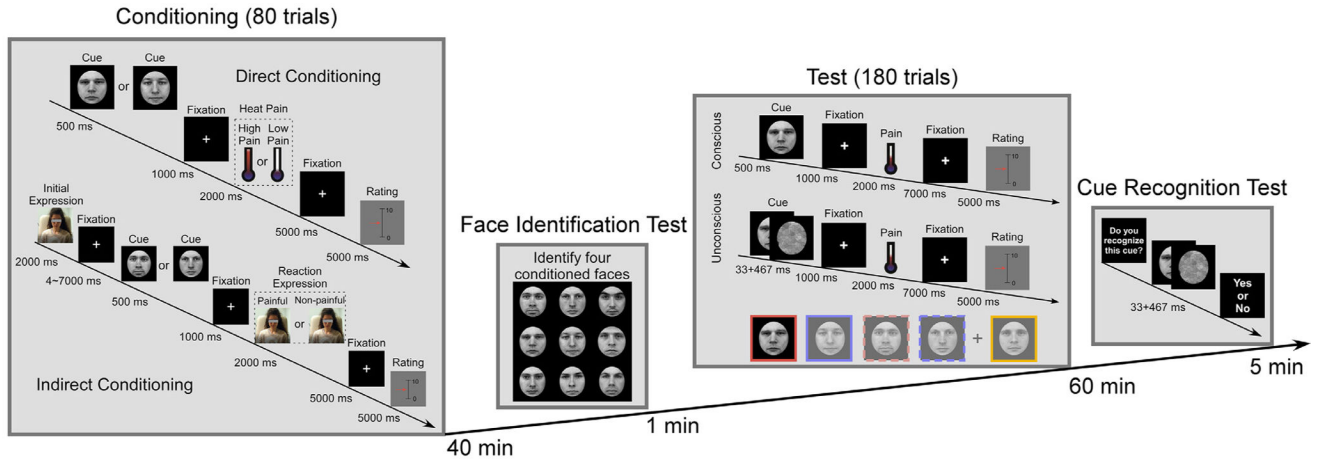
Acknowledgements

References

Atlas LY, Bolger N, Lindquist MA, Wager TD, 2010. Brain mediators of predictive cue effects on perceived pain. J. Neurosci 30, 12964–12977. doi: 10.1523/JNEU-ROSCI.0057-10.2010. [PubMed: 20881115]

Atlas LY, Wager TD, 2012. How expectations shape pain. Neurosci. Lett 520, 140–148. doi: 10.1016/j.neulet.2012.03.039. [PubMed: 22465136]

Besson G, Barragan-Jason G, Thorpe SJ, Fabre-Thorpe M, Puma S, Ceccaldi M, Barbeau EJ, 2017. From face processing to face recognition: comparing three different processing levels. Cognition 158, 33–43. doi: 10.1016/j.cognition.2016.10.004. [PubMed: 27776224]

Boly M, Balteau E, Schnakers C, Degueldre C, Moonen G, Luxen A, Phillips C, Peigneux P, Maquet P, Laureys S, 2007. Baseline brain activity fluctuations predict somatosensory perception in humans. Proc. Natl. Acad. Sci. U. S. A 104, 12187–12192. doi: 10.1073/pnas.0611404104. [PubMed: 17616583]

Bosma RL, Kim JA, Cheng JC, Rogachov A, Hemington KS, Osborne NR, Oh J, Davis KD, 2018. Dynamic pain connectome functional connectivity and oscillations reflect multiple sclerosis pain. Pain 159, 2267–2276. doi: 10.1097/j.pain.0000000000001332. [PubMed: 29994989]

Buzsaki G, 2006. Rhythms of the brain, rhythms of the brain 10.1093/acprof:oso/9780195301069.001.0001

Chang C, Lin C, 2011. LIBSVM: a library for support vector machines. ACM Trans. Intell. Syst. Technol 2, 27.

Chapman CR, Casey KL, Dubner R, Foley KM, Gracely RH, Reading AE, 1985. Pain measurement: an overview. Pain 22, 1–31. doi: 10.1016/0304-3959(85)90145-9. [PubMed: 4011282]

Cichy RM, Pantazis D, Oliva A, 2014. Resolving human object recognition in space and time. Nat. Neurosci 17, 455–462. doi: 10.1038/nn.3635. [PubMed: 24464044]

Colloca L, Benedetti F, 2009. Placebo analgesia induced by social observational learning. Pain 144, 28–34. doi: 10.1016/j.pain.2009.01.033. [PubMed: 19278785]

Dale AM, Liu AK, Fischl BR, Buckner RL, Belliveau JW, Lewine JD, Halgren E, 2000. Dynamic statistical parametric mapping: combining fMRI and MEG for high-resolution imaging of cortical activity. Neuron 26, 55–67. [PubMed: 10798392]

Dehaene S, Changeux JP, 2011. Experimental and theoretical approaches to conscious processing. Neuron 70, 200–227. doi: 10.1016/j.neuron.2011.03.018. [PubMed: 21521609]

Dobs K, Isik L, Pantazis D, Kanwisher N, 2019. How face perception unfolds over time. Nat. Commun 10, 1258. doi: 10.1038/s41467-019-09239-1. [PubMed: 30890707]

Egorova N, Park J, Orr SP, Kirsch I, Gollub RL, Kong J, 2015. Not seeing or feeling is still believing: conscious and non-conscious pain modulation after direct and observational learning. Sci. Rep 5, 1–9. doi: 10.1038/srep16809.

Fields HL, 2018. How expectations influence pain. Pain 159, S3–S10. doi: 10.1097/j.pain.0000000000001272. [PubMed: 30113941]

Finniss DG, Kaptchuk TJ, Miller F, Benedetti F, 2010. Biological, clinical, and ethical advances of placebo effects. Lancet 375, 686–695. doi: 10.1016/S0140-6736(09)61706-2. [PubMed: 20171404]

Freeman S, Yu R, Egorova N, Chen X, Kirsch I, Claggett B, Kaptchuk TJ, Gollub RL, Kong J, 2015. Distinct neural representations of placebo and nocebo effect. Neuroimage 112, 197–207. doi: 10.1016/j.neuroimage.2015.03.015. [PubMed: 25776211]

Goeleven E, De Raedt R, Leyman L, Verschuere B, 2008. The Karolinska directed emotional faces: a validation study. Cognt. Emot 22, 1094–1118. doi: 10.1080/02699930701626582.

Gracely RH, McGrath F, Dubner R, 1978. Ratio scales of sensory and affective verbal pain descriptors. Pain 5, 5–18. [PubMed: 673440]

Haufe S, Meinecke F, Görgen K, Dähne S, Haynes J–D, Blankertz B, Bießmann F, 2014. On the interpretation of weight vectors of linear models in multivariate neuroimaging. Neuroimage 87, 96–110. doi: 10.1016/J.NEUROIMAGE.2013.10.067. [PubMed: 24239590]

Hayes AF, Preacher KJ, 2014. Statistical mediation analysis with a multi-categorical independent variable. Br. J. Math. Stat. Psychol 67, 451–470. doi: 10.1111/bmsp.12028. [PubMed: 24188158]

Hu L, Iannetti GD, 2019. Neural indicators of perceptual variability of pain across species. Proc. Natl. Acad. Sci 116, 1782–1791. doi: 10.1073/pnas.1812499116. [PubMed: 30642968]

Huang MX, Mosher JC, Leahy RM, 1999. A sensor-weighted overlapping-sphere head model and exhaustive head model comparison for MEG. Phys. Med. Biol 44, 423–440. doi: 10.1088/0031-9155/44/2/010. [PubMed: 10070792]

Hunter T, Siess F, Colloca L, 2014. Socially induced placebo analgesia: a comparison of a pre-recorded versus live face-to-face observation. Eur. J. Pain 18, 914–922. doi: 10.1002/j.1532-2149.2013.00436.x. [PubMed: 24347563]

Jensen KB, Kaptchuk TJ, Chen X, Kirsch I, Ingvar M, Gollub RL, Kong J, 2015. A neural mechanism for nonconscious activation of conditioned placebo and nocebo responses. Cereb. Cortex 25, 3903–3910. doi: 10.1093/cercor/bhu275. [PubMed: 25452576]

Jensen KB, Kaptchuk TJ, Kirsch I, Raicek J, Lindstrom KM, Berna C, Gollub RL, Ingvar M, Kong J, 2012. Nonconscious activation of placebo and nocebo pain responses. Proc. Natl. Acad. Sci 109, 15959–15964. doi: 10.1073/pnas.1202056109. [PubMed: 23019380]

Kaptchuk TJ, Kelley JM, Conboy LA, Davis RB, Kerr CE, Jacobson EE, Kirsch I, Schyner RN, Nam BH, Nguyen LT, Park M, Rivers AL, McManus C, Kokkotou E, Drossman DA, Goldman P, Lembo AJ, 2008. Components of placebo effect: randomised controlled trial in patients with irritable bowel syndrome. BMJ 336, 999–1003. doi: 10.1136/bmj.39524.439618.25. [PubMed: 18390493]

Kim JA, Bosma RL, Hemington KS, Rogachov A, Osborne NR, Cheng JC, Oh J, Dunkley BT, Davis KD, 2020. Cross-network coupling of neural oscillations in the dynamic pain connectome reflects chronic neuropathic pain in multiple sclerosis. NeuroImage Clin 26, 102230. doi: 10.1016/j.nicl.2020.102230. [PubMed: 32143136]

King J–R, Dehaene S, 2014. Characterizing the dynamics of mental representations: the temporal generalization method. Trends Cogn. Sci 18, 203–210. doi: 10.1016/j.tics.2014.01.002. [PubMed: 24593982]

King J–R, Pescetelli N, Dehaene S, 2016. Brain mechanisms underlying the brief maintenance of seen and unseen sensory information. Neuron 92, 1122–1134. doi: 10.1016/j.neuron.2016.10.051. [PubMed: 27930903]

Kober H, Barrett LF, Joseph J, Bliss-Moreau E, Lindquist K, Wager TD, 2008. Functional grouping and cortical–subcortical interactions in emotion: a meta-analysis of neuroimaging studies. Neuroimage 42, 998–1031. doi: 10.1016/J.NEUROIMAGE.2008.03.059. [PubMed: 18579414]

Kong J, Benedetti F, 2014. Placebo and nocebo effects: an introduction to psychological and biological mechanisms. Handb Exp Pharmacol 225, 2–15.

Kong J, Kaptchuk TJ, Polich G, Kirsch I, Vangel M, Zyloney C, Rosen B, Gollub RL, 2009. An fMRI study on the interaction and dissociation between expectation of pain relief and acupuncture treatment. Neuroimage 47, 1066–1076. doi: 10.1016/j.neuroimage.2009.05.087. [PubMed: 19501656]

Kong J, Wang Z, Leiser J, Minicucci D, Edwards R, Kirsch I, Wasan AD, Lang C, Gerber J, Yu S, Napadow V, Kaptchuk TJ, Gollub RL, 2018. Enhancing treatment of osteoarthritis knee pain by boosting expectancy: A functional neuroimaging study. Neuroimage Clin 18, 325–334. [PubMed: 29868449]

Kucyi A, Davis KD, 2015. The dynamic pain connectome. Trends Neurosci 38, 86–95. doi: 10.1016/j.tins.2014.11.006. [PubMed: 25541287]
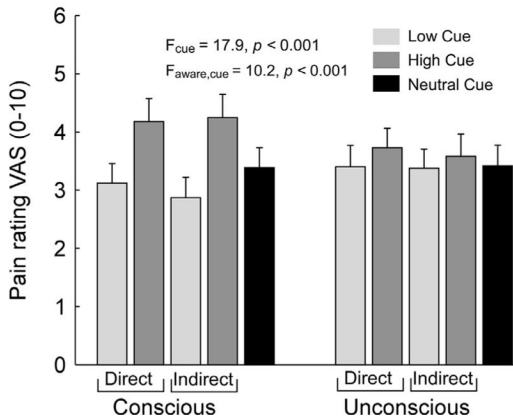
Lau HC, Passingham RE, 2006. Relative blindsight in normal observers and the neural correlate of visual consciousness. Proc. Natl. Acad. Sci 103, 18763–18768. doi: 10.1073/pnas.0607716103. [PubMed: 17124173]

Maris E, Oostenveld R, 2007. Nonparametric statistical testing of EEG- and MEG-data. J. Neurosci. Methods 164, 177–190. doi: 10.1016/j.jneumeth.2007.03.024. [PubMed: 17517438]

Melloni L, Molina C, Pena M, Torres D, Singer W, Rodriguez E, 2007. Synchronization of neural activity across cortical areas correlates with conscious perception. J. Neurosci 27, 2858–2865. doi: 10.1523/JNEUROSCI.4623-06.2007. [PubMed: 17360907]

Moncrieff J, Kirsch I, 2005. Efficacy of antidepressants in adults. BMJ 331, 155–157. doi: 10.1136/bmj.331.7509.155. [PubMed: 16020858]

Nakatani C, Raffone A, van Leeuwen C, 2014. Efficiency of conscious access improves with coupling of slow and fast neural oscillations. J. Cogn. Neurosci 26, 1168–1179. doi: 10.1162/jocn_a_00540. [PubMed: 24345169]

Pantazis D, Fang M, Qin S, Mohsenzadeh Y, Li Q, Cichy RM, 2018. Decoding the orientation of contrast edges from MEG evoked and induced responses. Neuroimage 180, 267–279. doi: 10.1016/J.NEUROIMAGE.2017.07.022. [PubMed: 28712993]

Pessiglione M, Petrovic P, Daunizeau J, Palminteri S, Dolan RJ, Frith CD, 2008. Subliminal instrumental conditioning demonstrated in the human brain. Neuron 59, 561–567. doi: 10.1016/j.neuron.2008.07.005. [PubMed: 18760693]

Pessiglione M, Schmidt L, Draganski B, Kalisch R, Lau H, Dolan RJ, Frith CD, 2007. How the brain translates money into force: a neuroimaging study of subliminal motivation. Science (80-.) 316, 904–906. doi: 10.1126/science.1140459.

Petrovic P, Kalso E, Petersson KM, Andersson J, Fransson P, Ingvar M, 2010. A prefrontal non-opioid mechanism in placebo analgesia. Pain 150, 59–65. doi: 10.1016/j.pain.2010.03.011. [PubMed: 20399560]

Salti M, Monto S, Charles L, King JR, Parkkonen L, Dehaene S, 2015. Distinct cortical codes and temporal dynamics for conscious and unconscious percepts. Elife 4, 1–52. doi: 10.7554/eLife.05652.

Schenk LA, Colloca L, 2020. The neural processes of acquiring placebo effects through observation. Neuroimage 209, 116510. doi: 10.1016/j.neuroimage.2019.116510. [PubMed: 31899287]

Shih Y–W, Tsai H–Y, Lin F–S, Lin Y–H, Chiang C–Y, Lu Z–L, Tseng M–T, 2019. Effects of positive and negative expectations on human pain perception engage separate but interrelated and dependently regulated cerebral mechanisms. J. Neurosci 39, 1261–1274. doi: 10.1523/JNEUROSCI.2154-18.2018. [PubMed: 30552181]

Sitt JD, King J–R, El Karoui I, Rohaut B, Faugeras F, Gramfort A, Cohen L, Sigman M, Dehaene S, Naccache L, 2014. Large scale screening of neural signatures of consciousness in patients in a vegetative or minimally conscious state. Brain 137, 2258–2270. doi: 10.1093/brain/awu141. [PubMed: 24919971]

Taulu S, Simola J, 2006. Spatiotemporal signal space separation method for rejecting nearby interference in MEG measurements. Phys. Med. Biol 51, 1759–1768. doi: 10.1088/0031-9155/51/7/008. [PubMed: 16552102]

Tu Y, Bi Y, Zhang L, Wei H, Hu L, 2020. Mesocorticolimbic pathways encode cue-based expectancy effects on pain. J. Neurosci 382–394. doi: 10.1523/JNEUROSCI.1082-19.2019. [PubMed: 31694965]

Tu Y, Park J, Ahlfors SP, Khan S, Egorova N, Lang C, Cao J, Kong J, 2018. A neural mechanism of direct and observational conditioning for placebo and nocebo responses. Neuroimage 184, 954–963. doi: 10.1016/J.NEUROIMAGE.2018.10.020. [PubMed: 30296557]

Tu Y, Zhang B, Cao J, Wilson G, Zhang Z, Kong J, 2019. Identifying inter-individual differences in pain threshold using brain connectome: a test-retest reproducible study. Neuroimage 202, 116049. doi: 10.1016/J.NEUROIMAGE.2019.116049. [PubMed: 31349067]

Tu Y, Zhang Z, Tan A, Peng W, Hung YS, Moayedi M, Iannetti GD, Hu L, 2016. Alpha and gamma oscillation amplitudes synergistically predict the perception of forthcoming nociceptive stimuli. Hum. Brain Mapp 37, 501–514. doi: 10.1002/hbm.23048. [PubMed: 26523484]

Vida MD, Nestor A, Plaut DC, Behrmann M, 2017. Spatiotemporal dynamics of similarity-based neural representations of facial identity. Proc. Natl. Acad. Sci 114, 388–393. doi: 10.1073/pnas.1614763114. [PubMed: 28028220]

Wager T, Scott DJ, Zubieta J–K, 2007. Placebo effects on human mu-opioid activity during pain. Proc. Natl. Acad. Sci 104, 11056–11061. 10.1073/pnas.89.6.2046 [PubMed: 17578917]

Wager TD, Atlas LY, 2015. The neuroscience of placebo effects: connecting context, learning and health. Nat. Rev. Neurosci 16, 403–418. doi: 10.1038/nrn3976. [PubMed: 26087681]

Wager TD, Rilling JK, Smith EE, Sokolik A, Casey KL, Davidson RJ, Kosslyn SM, Rose RM, Cohen JD, 2004. Placebo-induced changes in FMRI in the anticipation and experience of pain. Science (80-.) 303, 1162–1167. doi: 10.1126/science.1093065.

Wechsler ME, Kelley JM, Boyd IOE, Dutile S, Marigowda G, Kirsch I, Israel E, Kaptchuk TJ, 2011. Active Albuterol or Placebo, Sham Acupuncture, or No Intervention in Asthma. N. Engl. J. Med 365, 119–126. doi: 10.1056/NEJMoa1103319. [PubMed: 21751905]

Wiech K, Ploner M, Tracey I, 2008. Neurocognitive aspects of pain perception. Trends Cogn. Sci 12, 306–313. doi: 10.1016/j.tics.2008.05.005. [PubMed: 18606561]

A Experimental design and timings

B Pain ratings after conditioned cues

$F_{cue} = 17.9$, $p < 0.001$
$F_{aware,cue} = 10.2$, $p < 0.001$

Low Cue
High Cue
Neutral Cue

C Magnitudes of placebo and nocebo effects

$F_{mode} = 7.8$, $p = 0.01$
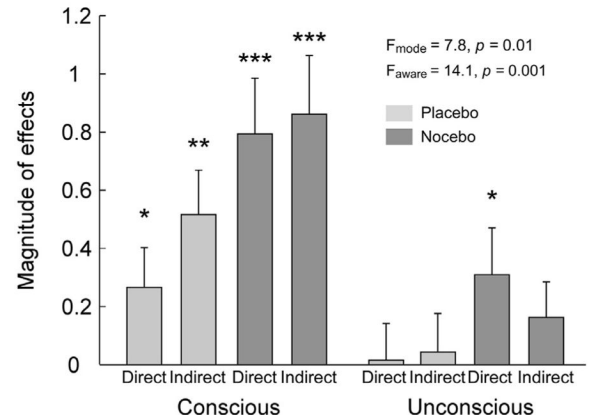$F_{aware} = 14.1$, $p = 0.001$

Placebo
Nocebo

Fig. 1. Experimental design and pain-related results.
A. This experiment consisted of two phases. In the conditioning phase (~40 mins), direct cues (faces with neutral expressions) were accompanied by heat pain stimulation of high or low intensity. Indirect cues (different faces with neutral expressions) were accompanied by observing a model experiencing high or low pain, showing both the physical reaction (painful or non-painful) and subjective pain ratings of the model. Each subject participated in both direct and indirect conditioning. At the end of the conditioning phase, the subjects were presented with a brief face identification test (~1 min). In the test phase (~60 mins), one of five cues (four learned cues from conditioning and one novel, neutral cue) appeared either supraliminally (500 ms) or subliminally (33 ms + 467 ms mask). The directly and indirectly conditioned high pain cues were presented with solid red and dashed red boxes, respectively. The directly and indirectly conditioned low pain cues were presented with solid blue and dashed blue boxes, respectively. The control cue was presented with a solid yellow box. Identical moderate pain stimuli (~2 s) followed all cues. Subjects were instructed to rate each stimulus on a 0–10 numerical rating scale. At the end of the test phase, a cue recognition test was presented (~5 mins). **B.** Pain ratings of identical moderate heat pain stimuli after conditioned predictive cues during the test phase. **C.** Magnitudes of directly and

indirectly conditioned placebo analgesia and nocebo hyperalgesia. Errorbars in B and C represent standard error of mean. $*p < 0.05$, $**p < 0.01$ and $***p < 0.001$.
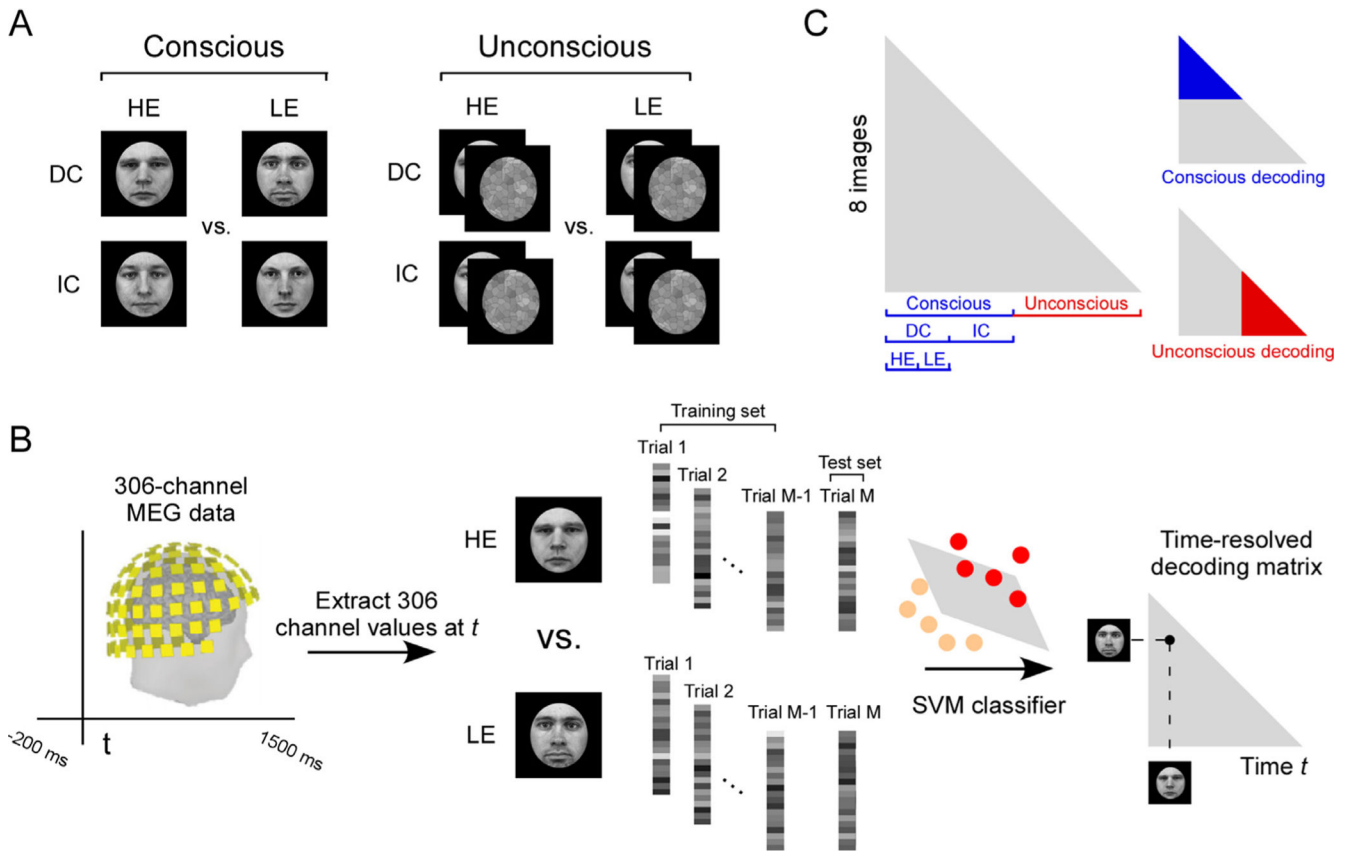
Fig. 2. Decoding cue-based expectancy from MEG signals.
A. Image sets of four conditioned face cues for conscious and unconscious trials. B.
Multivariate pattern analyses were performed in a time-resolved manner on MEG data
extracted from all sensors. For each time point t, we extracted MEG data for each face cue
and each trial and performed pairwise cross-validated SVM classification. C. The resulting
decoding accuracy values resulted in an 8×8 symmetric decoding matrix for each time
point. HE: high expectation cue; LE: low expectation cue; DC: direct conditioning; IC:
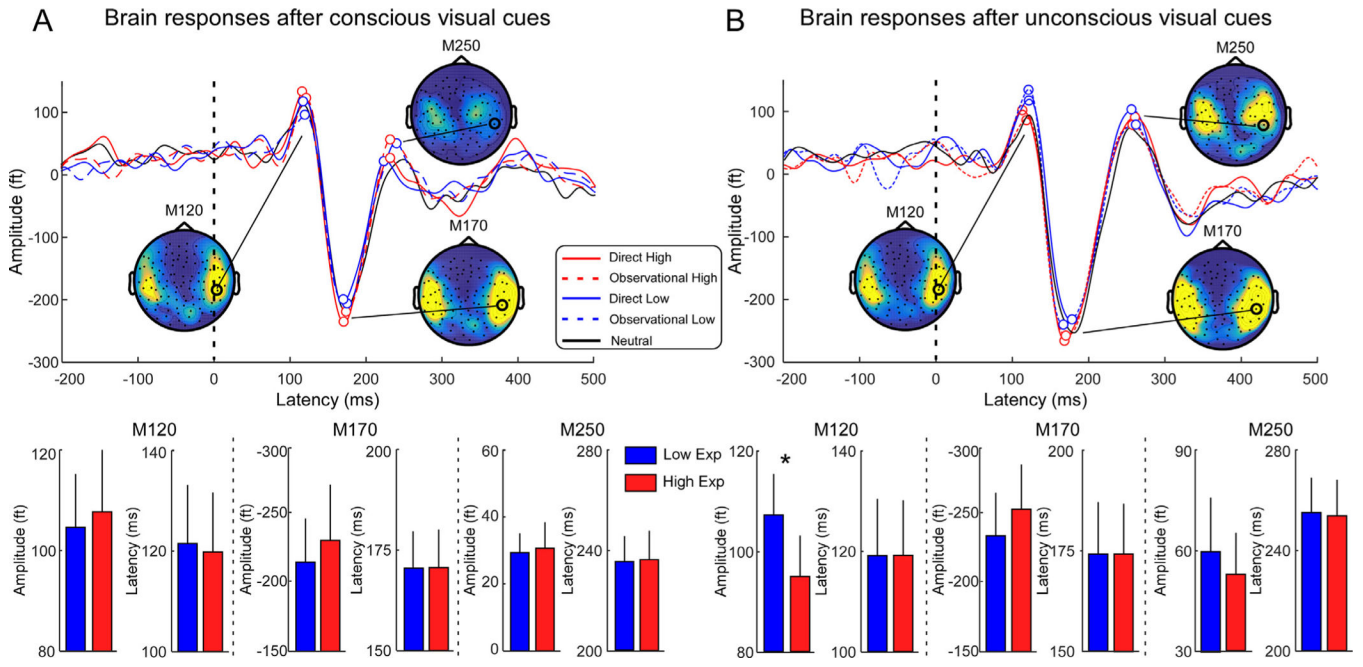indirect conditioning.

Fig. 3. Brain responses after consciously and unconsciously perceived visual cues.
Three prominent deflections were identified: M120, M170, and M250, with peaks around 120, 170, and 250 ms after stimulus onset, respectively. They all showed the largest magnitudes at bilateral temporal regions. Repeated-measures ANOVA showed a significant effect of cue on the magnitudes of M120 after unconsciously perceived face cues ($p = 0.04$). No significant differences in peak latency for any of the three deflections were found in the consciously or unconsciously perceived cues.
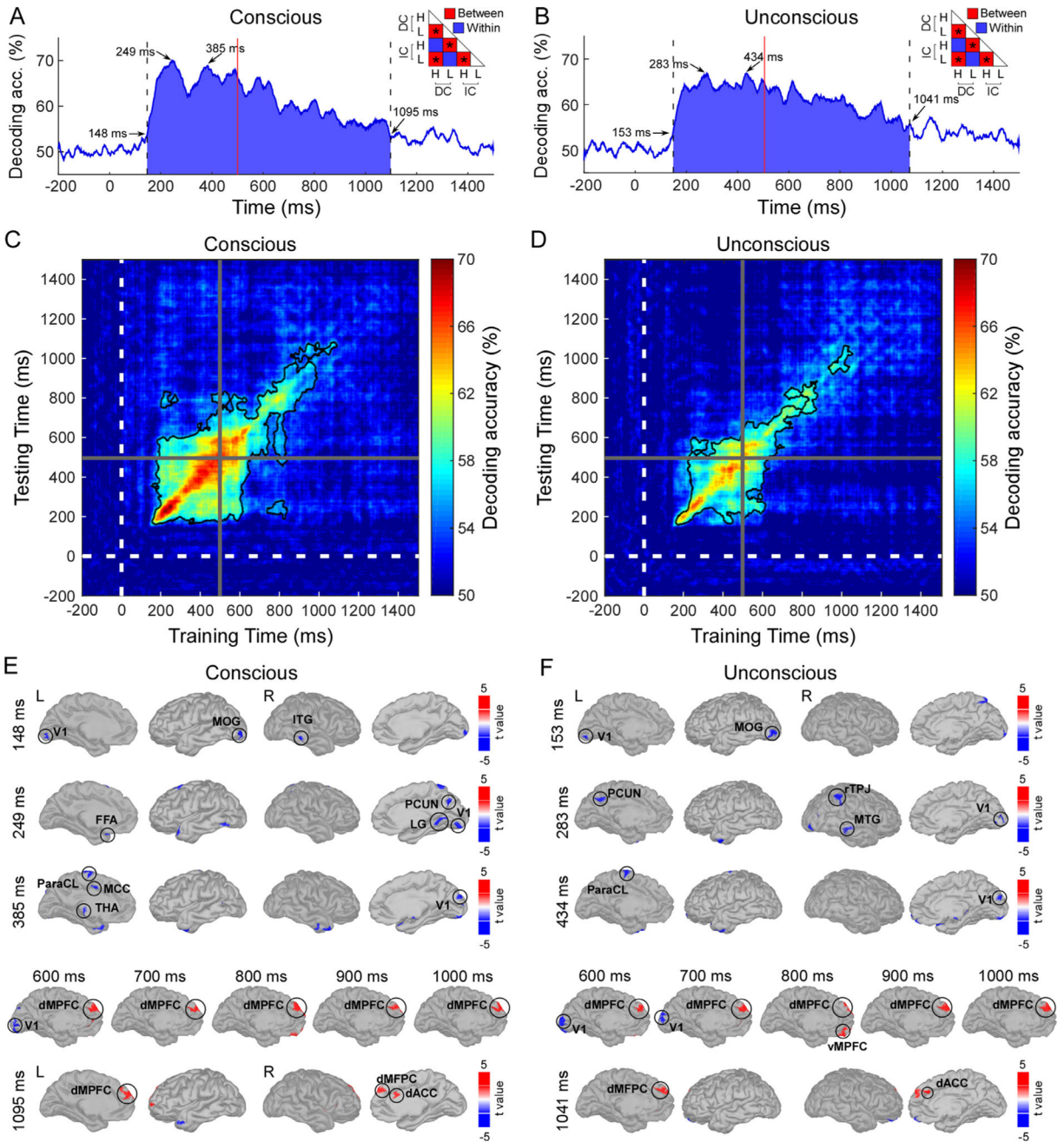
Fig. 4. Decoding consciously and unconsciously perceived high and low pain cues.
A and B: Time course of decoding high and low pain cues from the average of four between-expectation pairs (as indicated by an asterisk). Shading and dashed lines indicate significant time clusters (cluster-corrected sign permutation test, cluster-defining threshold $p < 0.05$, corrected significance level $p < 0.05$). The red line marks cue offset ($t = 500$ ms). Please note that we were not able to perform decoding across conscious and unconscious cues since the effect would be driven by the masking image. **C and D:** Temporal generalization of decoding high and low pain cues. The black contour indicates significant decoding area (cluster-corrected sign permutation test, cluster-defining threshold $p < 0.001$,

corrected significance level $p < 0.05$). The white dashed line and gray solid line mark the cue onset and offset times, respectively. **E and F:** Spatiotemporal regions in cortical sources with significant contribution in decoding high and low pain cues ($p < 0.001$ uncorrected and $p < 0.05$ FDR corrected). Brain responses that were greater after a low cue than a high cue are shown in blue, while those that were greater after a high cue than a low cue are shown in red. V1: primary visual cortex, ITG: inferior temporal gyrus, FFA: fusiform area, PCUN: precuneus, LG: lingual gyrus, ParaCL: paracentral lobule, MCC: middle cingulate cortex, THA: thalamus, dMFPC: dorsal medial prefrontal cortex, dACC: dorsal anterior cingulate cortex, rTPJ: right temporoparietal junction, MTG: middle temporal gyrus, vMPFC: ventromedial prefrontal cortex.
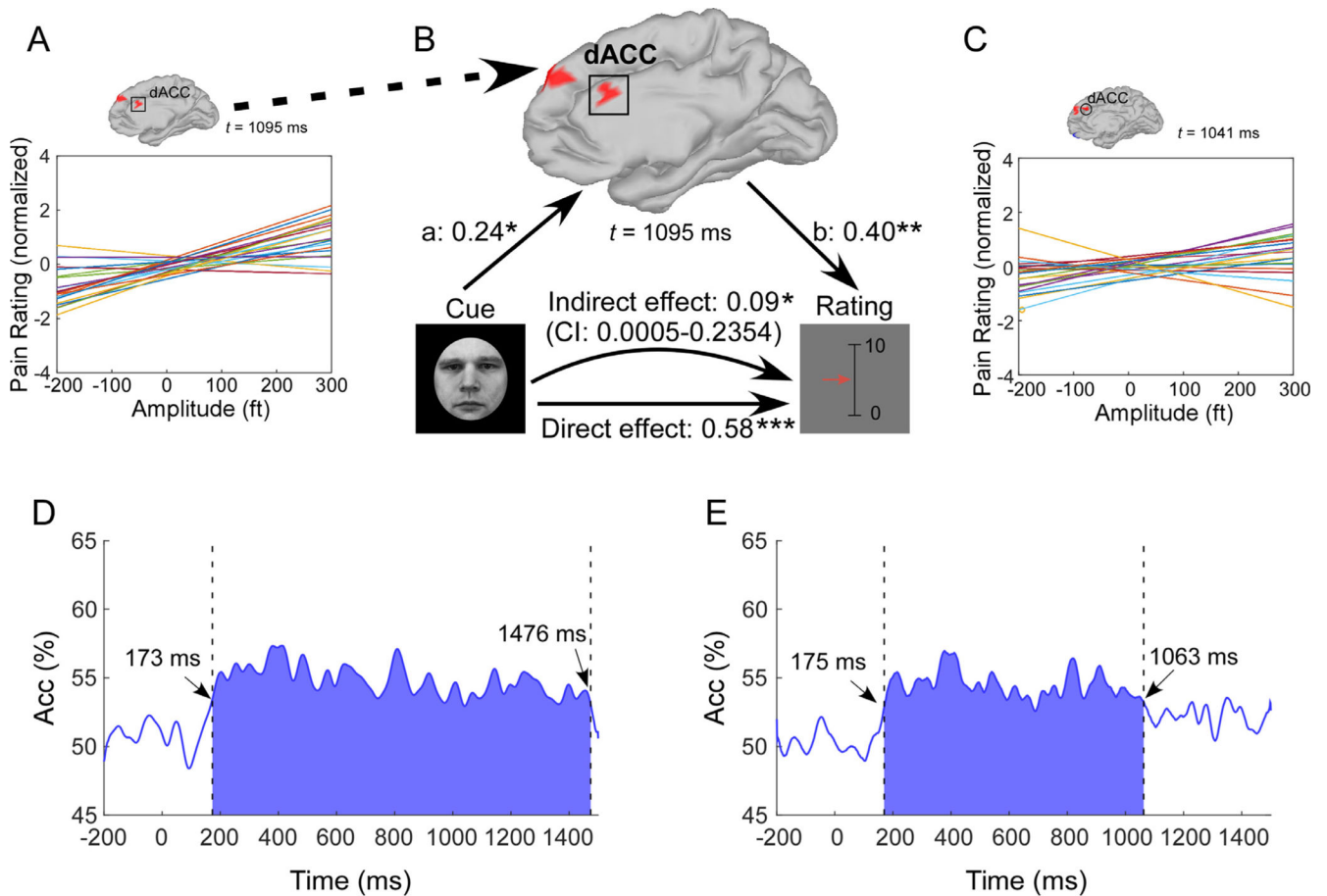
Fig. 5. Associations between spatiotemporal dynamics and pain.
A. After consciously perceived cues, brain responses in the dorsal anterior cingulate cortex (dACC) at 1095 ms were positively correlated with pain intensities (normalized across subjects). Each colored line indicates an individual subject. **B.** At single-subject level, consciously perceived cue-based expectancy on pain intensities was mediated by brain responses in the dACC at 1095 ms. *: $p < 0.05$, **: $p < 0.01$, ***: $p < 0.001$. **C.** After unconsciously perceived cues, brain responses in the dorsal anterior cingulate cortex (dACC) at 1041 ms were positively correlated with pain intensities (normalized across subjects). Each colored line indicates an individual subject. **D and E.** Predicting pain levels (high vs. low) using anticipatory MEG. Shading and dashed lines indicate significant prediction cluster (cluster-corrected sign permutation test, cluster-defining threshold $p < 0.05$, corrected significance level $p < 0.05$).